Experimental measurement of angular and overlap dependence of conduction between carbon nanotubes of identical chirality and diameter

Chris J. Barnett,[1] Christopher Evans,[2] James E. McCormack,[1] Cathren E. Gowenlock,[1] Peter Dunstan,[2] W. Wade Adams,[3] Alvin Orbaek White,[1] and Andrew R. Barron[1,3,4]*

[1]Energy Safety Research Institute, Swansea University, Bay Campus, Swansea, SA1 8EN, Wales, UK.

[2]Department of Physics, College of Science, Swansea University, Singleton Park, Swansea SA2 8PP, UK.

[3]Department of Materials Science and Nanoengineering, Rice University, Houston, Texas 77007, USA.

[4]Department of Chemistry, Rice University, Houston, Texas 77007, USA.

*e-mail: a.r.barron@swansea.ac.uk, arb@rice.edu.

ABSTRACT: Measurement of the angular and overlap dependence of the conduction between two identical carbon nanotubes (CNTs), with the same diameter and chirality, has only been possible through theoretical calculations; however, our observation of increased resistance adjacent to the junction between two CNTs facilitates such measurements. Since electrical resistance was found to increases with increased diameter ratio, applying 10 V to one of dissimilar diameter CNTs results in cleavage at the junction. Manipulation of the resulting identical CNTs (created by cutting a single CNT) allows for the direct measurement of the angular and parallel overlap conduction. Angular ($13<\theta<63°$) dependence shows two minima (22° and 24°) and a maximum at 30°, and conduction between parallel CNTs increases with overall tip separation, but shows a sinusoidal relationship with contact length, consistent with the concept of atomic scale registry.

KEYWORDS: *Multi-walled carbon nanotubes, manipulation, resistance, conduction*

Understanding the factors that control conduction between carbon nanotubes (CNTs) is fundamental to the optimization of CNT fiber conductors,[1] which offer potential as a lightweight replacement for copper.[2,3] The performance of CNT fiber conductors has been shown to depend on the purity of the CNTs, the addition of dopants, and the density of the fiber.[1,4] The latter is usually associated with alignment of the CNTs; contrarily, the electrical resistivity in the direction perpendicular to the CNT in a bundle or fiber can be several times higher than that in the parallel direction, [5,6] and the electrical resistivity in a disordered mat of CNTs was found to be 20x than that of its constituent CNTs.[7] Computational studies show that there is a significant angular dependence for the conductivity between two crossed single walled carbon nanotubes (SWCNTs), that varies whether identical or different chiralities are considered.[8,9] The optimum conduction is proposed to be related to the alignment of the 6-member rings within the CNTs. Unfortunately, obtaining experimental verification of this effect is fraught with difficulties, not the least the statistically negligible chance of picking two CNTs with the same diameter and chirality from any batch, because SWCNTs exist as dozens of chiralities and associated diameters, while MWCNTs have the additional complication of variations in the number of side walls: making it essentially impossible to pick two identical CNTs from a sample.[10,11] Nevertheless, a measurement of the contact resistance versus angle for multi walled carbon nanotubes-highly oriented pyrolytic graphite (MWCNT-HOPG) interfaces showed that there was a periodic relationship with minimum resistance at 0°, 60°, 120° and 180° clearly associated with the C_6 cyclic structure, plus another minimum ~25°.[12] We have recently undertaken detailed 2-point probe measurements of the electrical properties of individual MWCNTs,[13] where the presence of a depletion zone surrounding the junction with the tip resulted in increased resistance when the tips were sufficiently close to allow overlap of the depletion zones (<4 μm). This observation led us to investigate if there was a similar depletion region at the junction of two CNTs when crossed.

MWCNTs were synthesized via chemical vapor deposition (CVD) using a table top horizontal tube reactor to heat a carbon source of toluene and ferrocene as an iron catalyst to 750 °C.[14] The MWCNTs were subjected to microwave irradiation followed by chlorine treatment to remove the majority of residual iron catalyst.[15] The MWCNTs synthesized were of varying lengths (<40 μm) and diameter (<200 nm) and were drop cast on to the native oxide of a Si wafer from ethanol suspensions. The substrate's resistivity was $>10^3$ higher than all the MWCNT measured. The sample was annealed in vacuum at 500 °C for one hour to increase the reproducibility of the contacts.[13] The 2-point probe measurements were obtained in an Omicron Lt Nanoprobe equipped with SEM column (base pressure 1 x 10^{-11} mbar) using tungsten STM probes that were etched in 2 M KOH solution,[16] and annealed under vacuum to minimize the effects of the shank oxide on the electrical measurements and to increase contact reproducibility.[17,18] The tips were manually approached onto the CNTs to prevent strain on the CNTs that could affect the resistance measurements.[19] For CNT crossing experiments, the first tip was landed on a nanotube at 2 μm away from any crossing points. The second tip was landed on the same nanotube at least 2 μm away on the other side of the crossing point. Voltage current spectra where collected by sweeping the voltage from -1 V to +1 V and 5 spectra where collected at each site. SEM beams can affect resistance measurements, therefore for during the collection of all IV measurements, the SEM beam is switched off. The second tip was then moved to manually approach the nanotube within 50 nm of the crossing point, and the IV measurements were repeated. Measurements were take also take on all sides of the cross as well as on the cross itself. Ten crossing points where measured in this way.

Figure 1 shows representative SEM images of two MWCNTs with the location of electrical measuring points along with the resistances measured at each point. Multiple measurements were taken along the MWCNT and all 2-point probe measurements were repeated 5 times at the same point with ±1 V bias using an Omicron Lt Nanoprobe (see

Supplementary Material). The resistance measured at ±1 V on the lower MWCNT away from a crossing point (Figure 1a and f) was of the order of 30 kΩ; however, when the tip was landed close to the crossing point the resistance increased to 80.5 kΩ (Figure 1b). This effect only occurred when the tip was landed on the lower of the two crossing carbon nanotubes. When resistance measurements are made of the MWCNT lying on top of the cross (Figure 1d), it was found that proximity to the cross did not affect the result, even when the probe was landed on top of the crossing point (Figure 1c). We attribute this increased resistance to a formation of a depletion region induced in the crossing area by the tubes which results in upwards band bending as the probe is brought into contact causing a more rectifying contact, this also indicates that the nanotube as semi-conducting.[13]

When there is a large miss match in the two MWCNT diameters, the increase in the resistance measured at the crossing point can be up to 3 orders of magnitude higher, with resistance near the crossing point being measured in the regions of MΩ compared with kΩ away from the crossing point (i.e., Figure 2a and b). Figure 2 shows the normalized I-V plots of two crosses where the nanotubes are of similar diameter and miss-matched diameter. From Figure 2e and f, the I-V plots measured close to the crossing point (red line) are more rectifying than those measured away from the crossing point (blue line). The contact also becomes more rectifying when the diameters of the crossing tubes are more dissimilar (i.e., Figure 2f). Figure 2g shows a graph of resistance ratio against the diameter ratio. The resistance ratio is the resistance measured at 1 V of the tube divided by the resistance measured at 1 V near the crossing point on the bottom tube. The diameter ratio was calculated by dividing the diameter of the lower tube by the diameter of the upper tube.

We believe the origin of the depletion region is electrostatic and is a result of the electron rich π-bonds repelling at the crossing point surfaces, creating a region devoid of electrons.[20,21] There is also the possibility that the small top tube allows for measurements to

be taken closer to the contact point of the cross therefore measuring at a location at the center of the depletion region; however, we do not believe this is the case as measurements on small similar diameter tubes give us the ability to measure very close to the point, and did not show higher resistances. Another possibility is that the high concentration of electrons on the surface of smaller diameter tubes results in a high electric field therefore creating a large depletion region.

To test if these areas of increased resistance near the crossing point of MWCNTs can result in electrical breakdown the probes were brought in contact with a nanotube on either side of a cross and the voltage swept to +10 V, as this voltage in known to break MWCNT.[22-24] Figure 3a shows the tips approached on nanotubes of similar diameter and Figure 3b shows the tips approached on two tubes of differing diameter. In both cases, after 10 V was applied both tubes suffer electrical breakdown. In the case where the probes were contacted near a cross of similar diameter the tube broke apart under the tip-nanotube contact point indicating the region of highest resistance, most likely due to contact resistance (Figure 3c). Where the probes are landed near a cross with tubes of differing diameter, the tube broke apart at a point of high resistance near the crossing point (marked in Figure 3d). It was found that running 10 V across the nanotube also results in the tip bonding to the two halves of the original MWCNT. This allows for manipulation of the tubes or in the case where the tube is on the bottom of the cross the removal of a section of the tube (see Supplementary Material). The most important result of this experiment is that *two* MWCNTs are created by cutting a *single* MWCNT; meaning that they are guaranteed to be the same diameter and chirality, also since the two halves of the tube are bonded (welded) to the tips, the contact between the tip and CNT does not change. This provides a *unique* experimental approach to confirm theoretical models of the angular and overlap dependence of the electrical conduction of CNT···CNT junctions.

Figure 4 shows the variation in the CNT···CNT contact resistance as a function of the crossing angle. The contact location was kept constant for all angles to ensure variation in surface did not affect the resistance measures, and as the tips are bonded to the CNTs contact resistance between the tips and CNTs does not change. The plot shows a similar double dip predicted by calculations for a junction between two (10,10) SWCNT, where the dips are proposed to be 60° apart and represent when the CNTs are in-registry, i.e., the C_6 rings are aligned.[8] As crossing angle is reduced the contact area increase therefore resistance will decrease, however for rigid tubes, of low diameter the change in contact area of the angle range measure will be negligible. Here, the MWCNTs appear "in-registry" at 22° and 44°. This would suggest that the concept of "in-registry" is looser for larger diameter MWCNTs as compared to idealized small diameter SWCNTs. We caution that the exact angle measurement is difficult to determine at the junction and it is inferred by the angles of the MWCNTs near the junction; however, there the angular dependence to the junction resistance is undisputed. It is interesting to note that the variation is ~3x; comparable to the theoretical values.[8] We have repeated the measurements with multiple samples and show similar results albeit with small shifts in the conduction minima as a function of junction angle.

It is also possible to manipulate the two halves of a cut MWCNT in a parallel manner (Figure 5a) to allow for the measurement of the conductance on the contact length, *l* (Figure 5b). Once arranged in a parallel manner the tips may be used to pull the MWCNTs apart while remaining attached, at 0.1 nm increments. It has previously been calculated that the dependence of conductance on *l* is nonlinear and quasiperiodic but the periods are different depending on the chirality of the CNTs: armchair = 3*a* and zig-zag = *a*, where *a* = the unit cell parameter.[8,9] As may be seen from Figure 5c, there is a general increase in resistance with increased distance consistent with an overall tip-to-tip separation as seen previously for individual MWCNTs. Over this is a clear periodic variation with a periodicity of ca. 2-3 Å, which is consistent with

an armchair unit cell (2.45 Å). The same periodicity was found in earlier experiments and theoretical calculations on the scanning tunneling microscopy images of nanotubes.[25] The data shows a noise overlaying the periodic variation, which we attribute to variations in alignment as one MWCNT is pulled with regard to the other. In order to confirm the periodic peaks from the noise, a Fast Fourier Transfer (FFT) was performed on 4 repeat measurements and the average FFT is shown in Figure 5d), the x-axis has been converted from the frequency domain to the special domain in to show the period, which can be seen to be 2.46 Å with another broader peak center between 4.5 Å and 5 Å which we attribute to the harmonic.

Employing the increased resistance at CNT···CNT junctions between dissimilar-diameter CNTs allows for a *unique* approach to the measurement of the electrical junction resistance between CNTs that are guaranteed to be of the same diameter and hence chirality, by cutting an individual CNT and manipulating the two halves.

Supporting Information

Experimental for 2-point probe measurements, additional SEM images for CNTs being manipulated, additional plot of resistance against crossing angle dependence, additional I-V plot, additional plot of resistance against displacement dependence, and videos for tubes being manipulated.

Author Contributions

The manuscript was written through contributions of all authors. All authors have given approval to the final version of the manuscript.

Notes

The authors declare no competing interests.

Acknowledgements:

Financial support was provided by the Welsh Government Sêr Cymru National Research Network in Advanced Engineering and Materials (NRN-150), the Sêr Cymru Chair Programme, the Office of Naval Research (N00014-15-2717), and the Robert A. Welch Foundation (C-0002). The Welsh Government is also acknowledged for Sêr Cymru II Fellowships (C.E.G. and A.O.W) part funded by the European Regional Development Fund (ERDF).

References

(1) Wilhite, P.; Vyas, A. A.; Tan, J.; Tan, J.; Yamada, T.; Wang, P.; Park, J.; Yang, C. Y. Metal–nanocarbon contacts. *Semicond. Sci. Technol.* **2014,** 29 054006.

(2) Anantram, M. P. Current-carrying capacity of carbon nanotubes, *Phys. Rev. B* **2000,** 62, R4837.

(3) Maiti, A.; Svizhenko, A.; Anantram, M. P. Electronic transport through carbon nanotubes: effects of structural deformation and tube chirality, *Phys. Rev. Lett*. **2002,** 88, 126805.

(4) Alvarenga, J.; Jarosz, P. R.; Schauerman, C. M.; Moses, B. T.; Landi, B. J.; Cress, C. D.; Raffaelle, R. P. High conductivity carbon nanotube wires from radial densification and ionic doping. *Appl. Phys. Lett.* **2010,** 97, 182106.

(5) Hone, J.; Llaguno, M. C.; Nemes, N. M.; Johnson, A. T. Electrical and thermal transport properties of magnetically aligned single wall carbon nanotube films. *Appl. Phys. Lett.* **2000,** 77, 666-668.

(6) Wang, X. B.; Liu, Y.Q.; Yu, G.; Xu, C. Y.; Zhang, J.B.; Zhu, D.B. Anisotropic electrical transport properties of aligned carbon nanotube films. *J. Phys. Chem. B* **2001,** 105, 9422-9425.

(7) Thess, A.; Lee, R.; Nikolaev, P.; Dai, H.; Petit, P.; Robert, J.; Xu, C.; Hee Lee, Y.; Gon Kim, S.; Rinzler, A. G.; et al. Crystalline ropes of metallic carbon nanotubes. *Science* **1996,** 273, 483-487.

(8) Buldum, A.; Lu, J. P. Contact resistance between carbon nanotubes. *Phys. Rev. B* **2001,** 63, 161403-1-161403-4.

(9) Xu, F.; Sadrzadeh, A.; Xu, Z.; Yakobson, B.I. Can carbon nanotube fibers achieve the ultimate conductivity? -Coupled-mode analysis for electron transport through the carbon nanotube contact. *J. Appl. Phys.* **2013,** 114, 063714.

(10) Liu, H.; Nishide, D.; Tanaka, T.; Kataura, H, Large-scale single-chirality separation of single-wall carbon nanotubes by simple gel chromatography. *Nat. Commun.* **2011,** 2, 309.

(11) Wei, X.; Tanaka, T.; Hirakawa, T.; Tsuzuki, M.; Wang, G.; Yomogida, Y.; Hirano, A.; Kataura, H. High-yield and high-throughput single-chirality enantiomer separation of single-wall carbon nanotubes. *Carbon* **2018,** 132, 1-7.

(12) Paulson, S.; Helser, A.; Buongiorno Nardelli, M.; Taylor, R. M.; Falvo1, M.; Superfine, R.; Washburn, S. Tunable resistance of a carbon nanotube–graphite interface. *Science* **2000,** 290, 1742-1744.

(13) Barnett, C. J.; Gowenlock, C.; Welsby, K.; Orbaek White, A.; Barron, A. R. Spatial and contamination dependent electrical properties of carbon nanotubes. *Nano Lett.* **2018,** 18, 695–700.

(14) Orbaek White, A.; Aggarwal, N.; Barron, A. R. The development of a 'process map' for the growth of carbon nanomaterials from ferrocene by injection CVD. *J. Mater. Chem. A* **2013,** 1, 14122-14132.

(15) Gomez, V.; Irusta, S.; Lawal, O. B.; Adams, W.; Hauge, R. H.; Dunnill, C. W.; Barron, A. R. Enhanced purification of carbon nanotubes by microwave and chlorine cleaning procedures. *RSC Adv.* **2016,** 6, 11895-11902.

(16) Ibe, J. P.; Bey Jr., P. P.; Brandow, S. L.; Brizzolara, R. A.; Burnham, N. A.; DiLella, D. P.; Lee, K. P.; Marrian, C. R. K.; Colton, R. J. On the electrochemical etching of tips for scanning tunnelling microscopy. *J. Vac. Sci. Technol. A* **1990,** 8, 3570-3575.

(17) Cobley, R. J.; Brown, R. A.; Barnett, C. J.; Maffeis, T. G. G.; Penny, M. W. Quantitative analysis of annealed scanning probe tips using energy dispersive X-ray spectroscopy. *Appl. Phys. Lett.* **2013,** 102, 023111.

(18) Barnett, C. J.; Kryvchenkova, O.; Wilson, L. S. J.; Maffeis, T. G. G.; Kalna, K.; Cobley, R. J. The role of probe oxide in local surface conductivity measurements. *J. Appl. Phys.* **2015,** 117, 174306.

(19) Smith, N. A.; Lord, A. M.; Evans, J. E.; Barnett, C. J.; Cobley, R. J.; Wilks, S. P. Forming reproducible non-lithographic nanocontacts to assess the effect of contact compressive strain in nanomaterials. *Semicond. Sci. Technol.* **2015,** 30, 065011.

(20) Warren, A. C.; Woodall, J. M.; Freeouf, J. L.; Grischkowsky, D.; McInturff, D. T. Arsenic precipitates and the semi-insulating properties of GaAs buffer layers grown by low-temperature molecular beam epitaxy. *Appl. Phys. Lett.* **1990,** 57, 1331-1333.

(21) Feenstra, R. M.; Dong, Y.; Semtsiv, M.; Masselink, W. Influence of tip-induced band bending on tunnelling spectra of semiconductor surfaces. *Nanotechnol.* **2006,** 18, 044015.

(22) Wang, M.; Wang, J.; Chen, Q.; Peng, L. Fabrication and electrical and mechanical properties of carbon nanotube interconnections. *Adv. Funct. Mater.* **2005,** 15, 1825-1831.

(23) Wei, X.; Yang, Y.; Chen, Q.; Wang, M.; Peng, L. The very low shear modulus of multi-walled carbon nanotubes determined simultaneously with the axial Young's modulus via in situ experiments. *Adv. Funct. Mater.* **2008,** 18, 1555-1562.

(24) Wei, X.; Chen, Q.; Liu, Y.; Peng, L. Cutting and sharpening carbon nanotubes using a carbon nanotube 'nanoknife'. *Nanotechnol.* **2007,** 18, 185503.

(25) Meunier, V.; Senet, P.; Lambin, P.; Scanning tunnelling spectroscopy signature of finite-size and connected nanotubes: A tight-binding study. *Phys. Rev. B* **1999,** 60, 7792-7795.

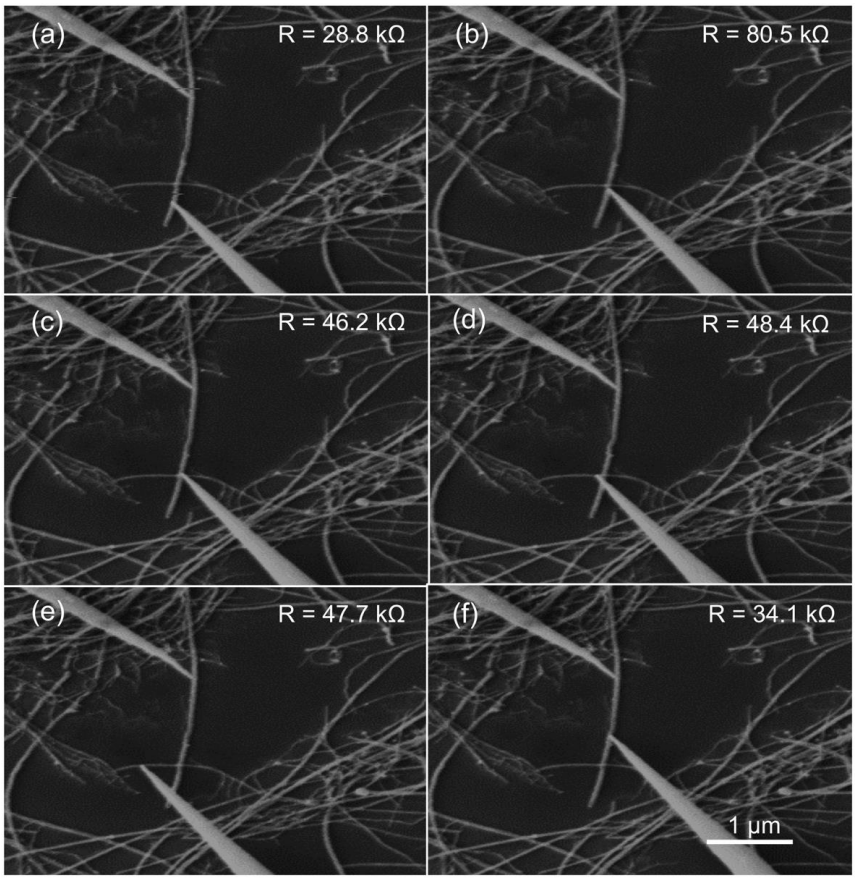

Figure 1. SEM images of measurements taken around a crossing point of two MWCNTs with the average resistance (@ 1 V) measured for each position. (a and f) are measured on the lower larger diameter MWCNT away from the junction; (b) is measured on the lower larger diameter MWCNT close to the junction; (c and d) are measured with one tip on the upper small diameter MWCNT; (e) is measured with one tip on the upper small diameter MWCNT away from the junction.

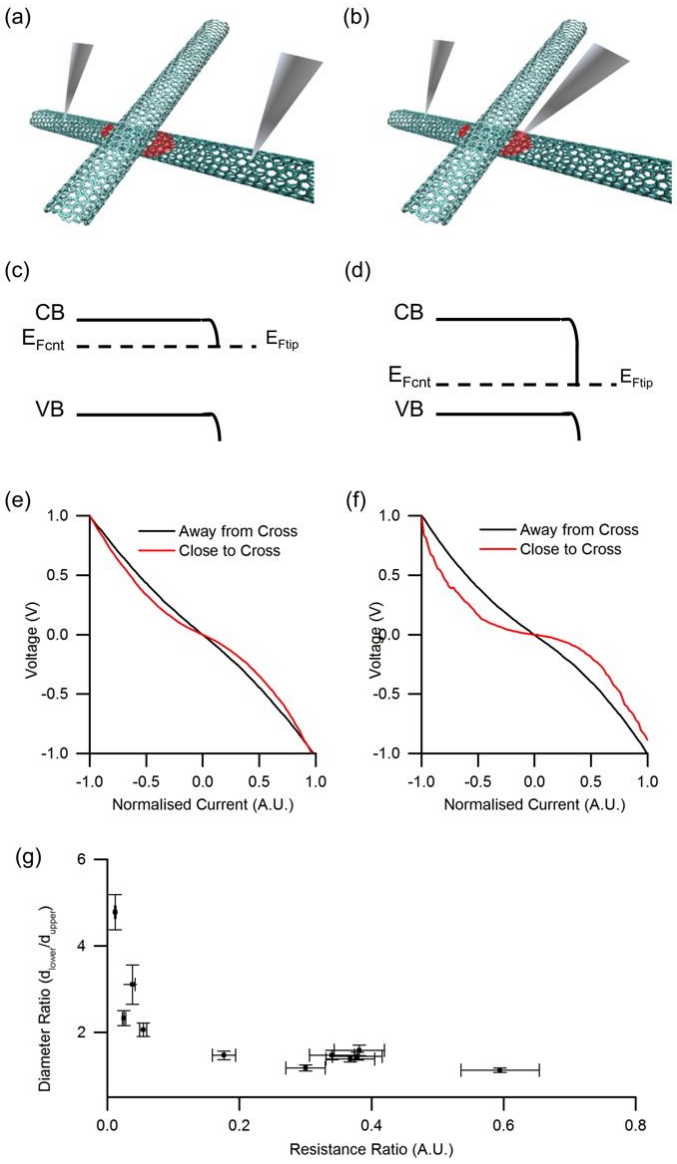

Figure 2. Diagram of crossing MWCNT showing depletion region (a and b), with associated band diagrams (c and d) showing upwards band bending when tip contacts the CNT, and normalized I-V curves of two MWCNTs of (e) similar diameter and (f) miss-matched diameter showing the measurement taken with the tips in the positions shown in (a) and (b), as blue and red lines, respectively. (g) Plot of diameter ratio for two crossed MWCNTs (d_{lower}/d_{upper}) as a function of ratio of the resistance measured of the MWCNT (a) and the resistance (@ 1 V) measured near the crossing point on the bottom tube (b). Error bars where calculated using the standard deviation from the 5 current measurements and propagated using the quotient rules and the uncertainty in the diameter measurements again and propagated using the quotient rules.

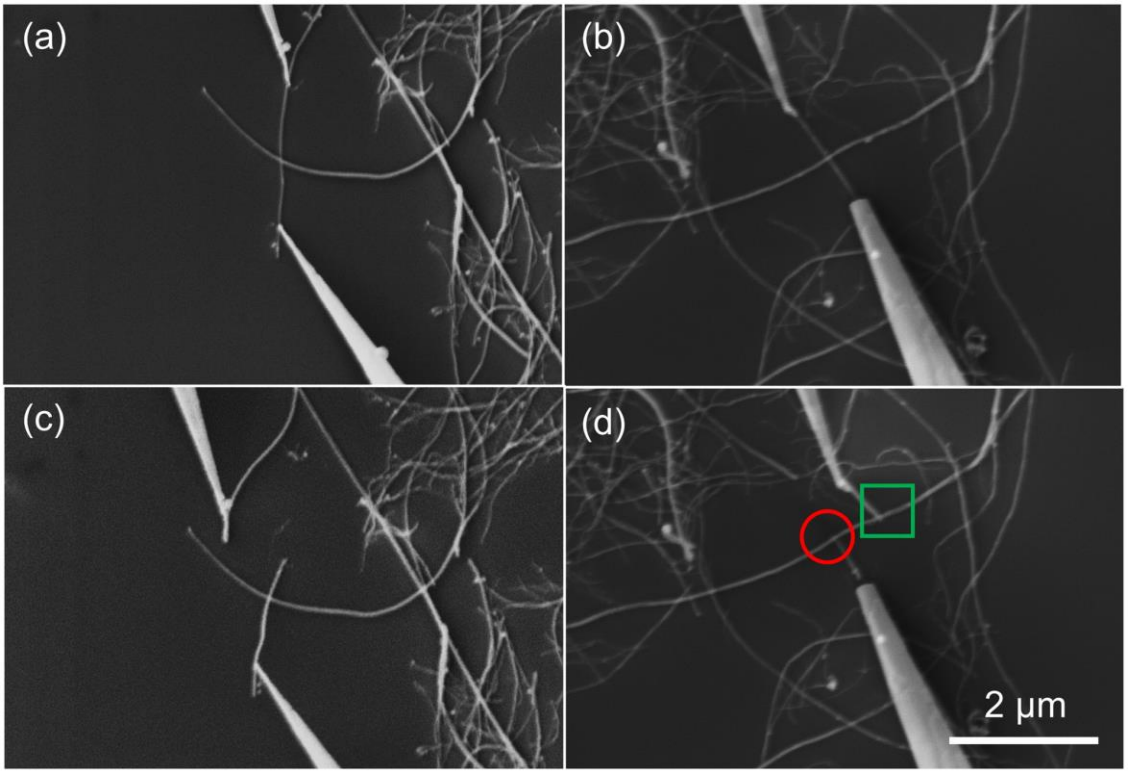

Figure 3. SEM images of tungsten probes positioned on a MWCNT crossing another MWCNT of (a) similar diameter and (b) of differing diameter, and after a voltage is swept from -10 V to 10 V through the MWCNT breakage occurs as shown in (c) and (d), respectively, showing the dependence on the breakage point of the variance in MWCNT diameter. The red circle and green square mark the breakage point.

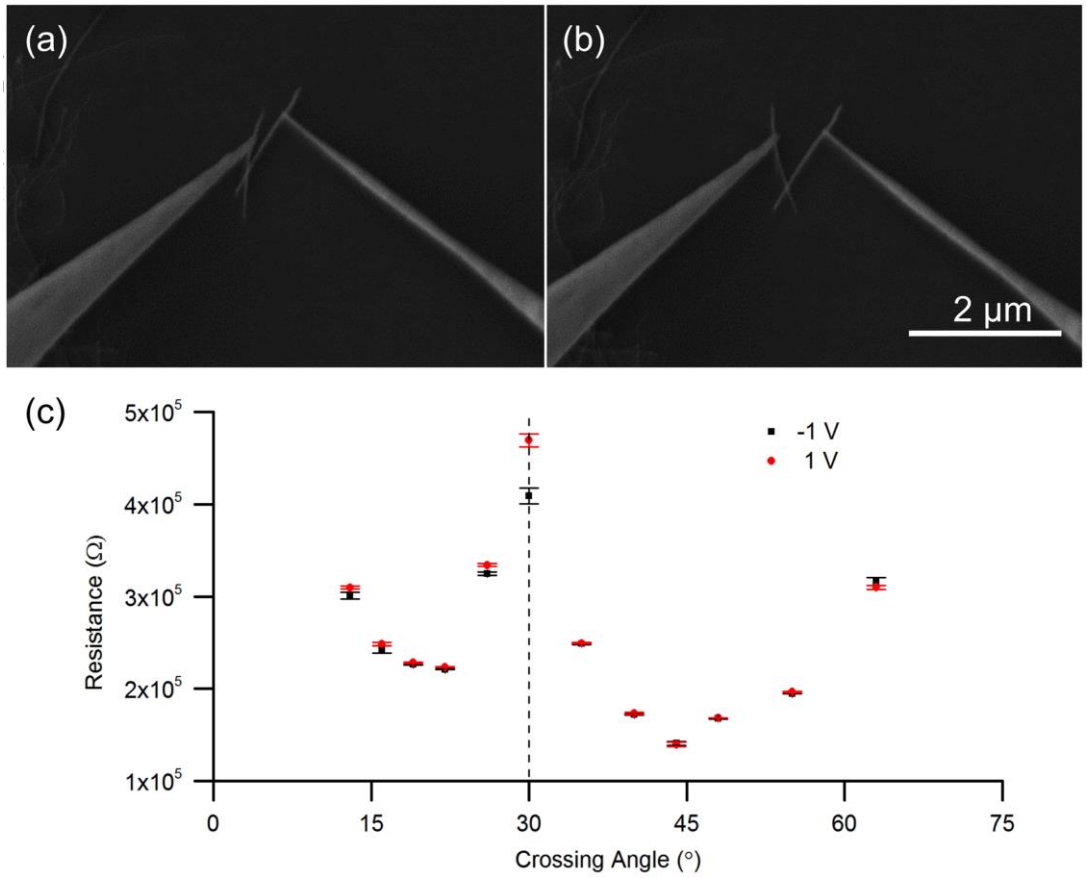

Figure 4. Series of SEM images (scale = 2 µm) showing the two parts of an individual MWCNT that has been cleaved and manipulated (see Supplementary Material) to create a crossed junction, where the angle can be altered to (a) 19° and (b) 55°. (c) Plot of resistance measured at +1 V and -1 V as a function of junction angle showing the angular dependence.

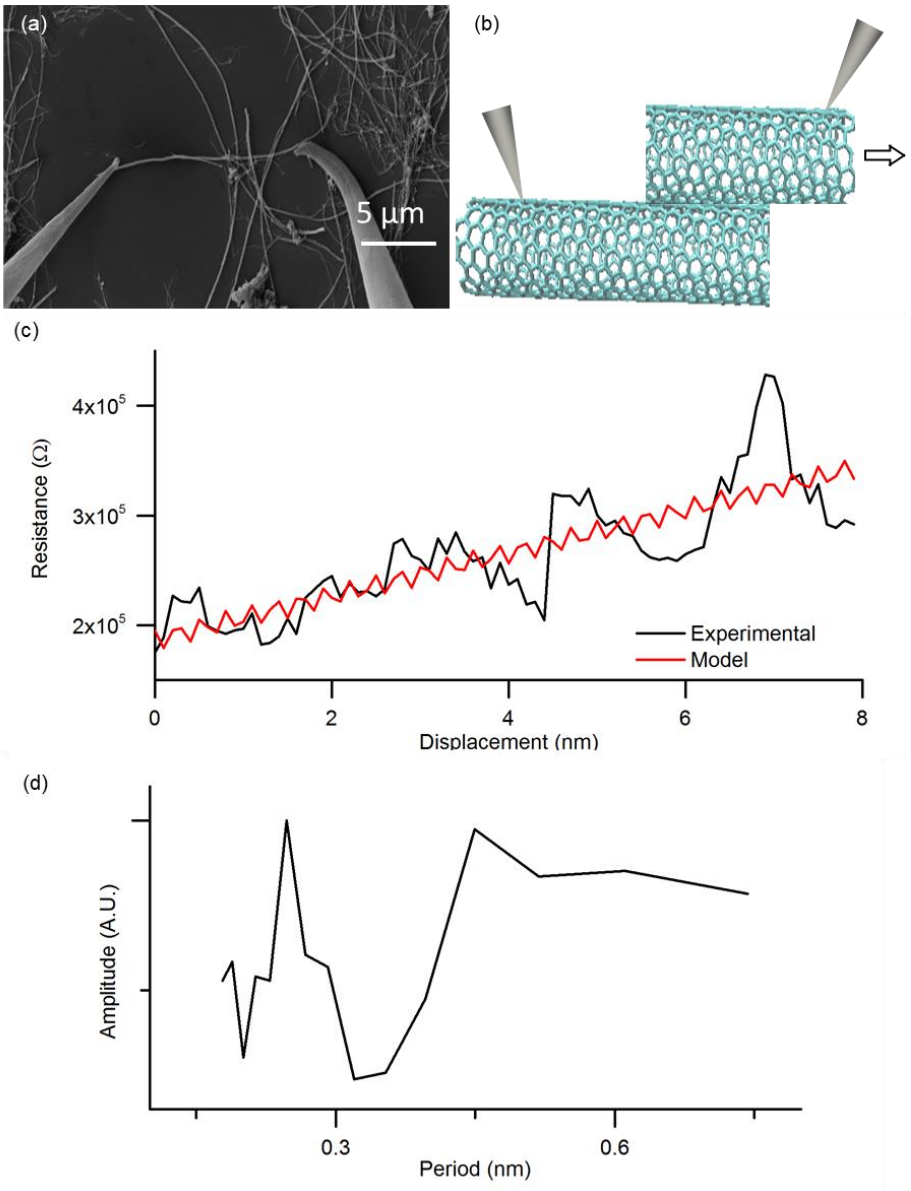

Figure 5. (a) SEM image two halves of the same nanotube manipulate to lie on top of each other as shown schematically in (b). (c) Plot of resistance measured at 1 V as a function of distance slid. The red line in (c) is based upon a simple model taking into account the periodicity of the lattice of CNTs and 0.1 nm drag of the top nanotube. The model is not intended to be an exact match of the experimental data but instead is to highlight the repeating features and peak shapes in the experimental data. (d) Plot of average FFT against period of the resistance against distance slid.

Graphical Abstract